Journal of Sol-Gel Science and Technology (2022) 104:503–511
https://doi.org/10.1007/s10971-022-05903-z

INVITED PAPER: FUNDAMENTALS OF SOL-GEL AND HYBRID MATERIALS PROCESSING

Investigation of local structures of silicon oxynitride glasses prepared from aerogels

Hiroyo Segawa[1,2] · Yuta Osawa[1,2] · Shunsuke Watanabe[1,2] · Shingo Machida[2] · Ken-ichi Katsumata[2] · Atsuo Yasumori[2] · Sadaki Samitsu[1] · Kenzo Deguchi[1] · Shinobu Ohki[1] · Naoki Ohashi[1]

Received: 5 April 2022 / Accepted: 4 July 2022 / Published online: 29 July 2022

Abstract

Oxynitride glasses in Si-Al-O-N system were synthesized to investigate atomic arrangements in those glasses. Aerogels of silica (SiO_2) and silica-alumina (SiO_2-Al_2O_3) system were fabricated by drying wet gels in supercritical CO_2 condition. The SiO_2 gels were prepared from the silicon alkoxide with CH_3 groups and the SiO_2-Al_2O_3 gels were prepared from silicone and aluminum alkoxides. Ammonolysis were performed at $T_N = 750$–1400 °C to synthesize oxynitride glasses. The nitrogen concentration in the resultant glasses increased with the increase in the ammonolysis temperatures and exceeded 34 eq.% by ammonolysis at 1300 °C. The specific surface area of these aerogels has been 1941 and 1159 $m^2\ g^{-1}$, respectively. The glass structures were investigated by adopting ^{29}Si and ^{27}Al NMR measurements. In silicon oxynitride glasses, it was revealed that only one N atom occupies the nearest neighbor site around Si after ammonolysis at $T_N < 1200$ °C, while two or more N atoms occupy the nearest neighbor site around Si after ammonolysis at $T_N > 1300$ °C. In Si-Al-O-N glasses, the number of N atoms at around neighboring to Si atom varied with ammonolysis temperature but any traces of Al-N bonds were not found, indicating the bridging N in the form of Si-N-Al was absent in the glasses.

Graphical Abstract

Nitrogen contents of oxynitride glasses prepared from silica-based aerogels with CH_3 groups (ON-CH_3) and those doped with Al and Eu ions (ON-AE) increased with increase of ammonolysis temperature. The ^{29}Si NMR spectra differed between ON-CH_3 and ON-AE.

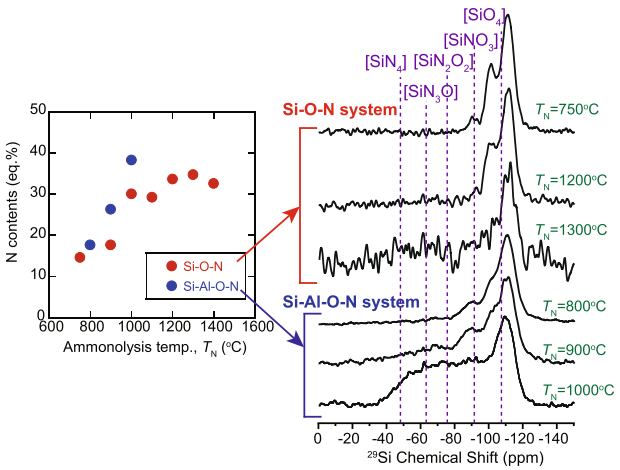

✉ Hiroyo Segawa
SEGAWA.Hiroyo@nims.go.jp

[1] National Institute of Materials Science, 1-1 Namiki, Tsukuba, Ibaraki 305-0044, Japan

[2] Tokyo University of Science, 6-3-1 Nijyuku, Katsushika-ku, Tokyo 125-8585, Japan

Keywords Aerogel · Oxynitride glasses · Pore distribution · NMR spectra · Glass structures

Highlights

- Silicon-based oxynitride glasses were prepared from aerogels via ammonolysis at high temperature.
- Nitrogen contents of the oxynitride glasses reached to higher than 34 eq.%.
- The local structures of the oxynitride glasses were investigated by ^{29}Si and ^{27}Al NMR measurements.
- It was found that most of inserted nitrogen was bonded to Si atoms.

1 Introduction

Oxynitride glasses, where a part of oxygen atoms in oxide glasses are replaced by nitrogen atoms, have been investigated over the last few decades. Particularly, a lot of attentions were paid to nitrogen incorporation into silicate or aluminosilicate glasses. Most of those studies focused on the physical properties such as hardness, Young's modulus, strength, toughness, refractive index, viscosity and glass transition temperature in relation with nitrogen substitution for oxygen [1–5]. Those silica-based oxynitride glasses were prepared by conventional melt-quenching method, where mixtures of oxides and nitrides were melted under low oxygen partial pressure conditions at high temperatures, e.g., $T \geq 1500$ °C. Many efforts are attempted to increase the nitrogen concentration in the silica-based oxynitride glasses synthesized by the melt quenching process. One of the strategies to increase the nitrogen concentration is the addition of extrinsic elements as glass modifiers. For instance, very high nitrogen concentration such as 65 eq.% was achieved by mixing pure metals or hydrides with conventional source materials as modifier for glass network structures [4, 6–9]. Here, the nitrogen concentration was calculated as equivalent concentration, N (eq.%) defined ad $(3[N] \times 100)/(3[N] + 2[O])$ where [N] and [O] are the concentration of nitrogen and oxygen, respectively [3]. The previous works represent that increasing nitrogen concentration in Si-O-N glasses without network modifiers is very difficult when melt-quench processes are adopted. Silicon nitride seems to be a useful precursor for preparation of Si-O-N glasses through melt quenching process but that is unlikely successful idea. Indeed, it is very hard to form stable Si-O-N melts with high nitrogen concentration because of the volatility of silicon nitride [10].

Because of the difficulty in the formation of melts with high nitrogen concentration, ammonolysis, that is, heating not molten salts but solid glasses under ammonia gas stream, has been considered as a way to synthesize Si-O-N glasses. By applying the ammonolysis, Brinker and Haaland synthesized dense, colorless and homogeneous glasses with up to 2 eq.% nitrogen in the Na-Al-Ba-Si-O-N system [11], and Rajaram and Day produced glasses in the M-Na-P-O-N system (M = alkaline earth element) with nitrogen contents up to 25 eq.% [12].

As ammonolysis involves gas/solid reaction, specific surface area of the precursor glass is, consequently, an essential parameter to govern the progress of nitridation. Hence, the usage of precursors with high specific surface area enables ammonolysis to occur at the low temperatures, e.g., $T < 1000$ °C [11, 13]. For instance, oxynitride glasses were successfully formed through ammonolysis of fibers and thin films prepared by sol-gel as precursors [14, 15]. However, successful preparation of the monolithic gels is known to be difficult since cracks were formed during the drying process of the gels [16]. Thus, the number of reports on fabrication of monolithic oxynitride glasses via sol-gel process has been limited [11, 17–19]. Szaniawska et al., reported that nitrogen was introduced into silica and SiO_2-B_2O_3 aerogels and the nitrided aerogels were converted to dense oxynitride glasses by heat treatment at 1600 °C in vacuum or in a nitrogen atmosphere [17, 18]. These results indicate that the nitridation of aerogels is a promising way to obtain monolithic oxynitride glasses since aerogels possess higher specific surface area than xerogels [20–23]. The most conventional process to prepare aerogels is drying wet gels under supercritical conditions: the residual solvents in wet gels can be removed without formation of cracks under supercritical conditions [22, 24, 25]. Needless to say, the efforts to prepare bulk oxynitride glasses without cracks is essentially important to evaluate their bulk properties of them, such as hardness and strength.

In these contexts, ammonolysis to doped silica gels were examined attempting to obtain monolithic oxynitride glasses [26, 27] and to verify the effects of gel structures upon the structure and properties of resultant oxynitride glasses. For instance, silica aerogels with CH_3 groups were employed as precursors for synthesis of Si-O-N glasses. Indeed, Si-O-N glasses without cracks were obtained after ammonolysis at $T > 1200$ °C, and nitrogen concentration in those glasses reached ~35 eq.%. The role of CH_3 groups in the precursor gels has been attributed to structural flexibility resulting from modification of Si-O network structure [23]. However, inhibition of crack generation by modification in Si-O network is not always the case. For instance, silica aerogels were crushed into chips even if they were doped

with approximately 1 at% Eu and Al ions. On the other hand, modification of pore size distribution and specific surface area seems to be effective for efficient nitridation by ammonolysis. Indeed, the nitrogen concentration in the glass obtained via ammonolysis of the aerogels doped with Eu and Al ions was relatively high, e.g., 38 eq.%. Those results indicated that the usage of modified or doped gels as precursors is an appropriate way to obtain oxynitride glasses with relatively high nitrogen concentrations but not always effective to prepare monolithic oxynitride glasses without cracks. In order to propose an effective strategy to obtain monolithic oxynitride glasses, it is necessary to understand the detailed mechanism of nitrogen insertion into aerogels and of crack generation.

As mentioned above, oxynitride glasses have been investigated as the formation of metal-nitrogen bonds is considered a possible way to improve the mechanical properties, such as hardness and toughness. Absolutely, the replacement of oxide ions by nitride ions should cause modification of the glass structures, such as coordination numbers and bonding strength, and those are considered as the origin of the changes in mechanical properties. Those structural modifications during nitridation are also a probable cause for crack generation during nitridation. Hence, in this study, we devoted ourselves to characterize the structures in oxynitride glasses prepared from aerogels via ammonolysis. In this study, we prepared the oxynitride glass specimens from silica gels with organic groups or with doped inorganic cations, and analyzed the glasses by nuclear magnetic resonance (NMR) and some other techniques, aiming to reveal the details of the nitridation induced by ammonolysis of silica-based aerogels.

2 Experimental

Two series of organically modified or ion-doped silica gels were prepared as the precursors for syntheses of oxynitride glasses in order to investigate the effect of modification in gel structures upon the structure of the resultant oxynitride glass structures. One is the silica gels with organic component, i.e., CH_3 groups, and the other is silica gels doped with inorganic components, i.e., Al and Eu ions, as modifiers for glass structures. Synthesis of SiO_2 gels with CH_3 groups was initiated with preparation of sols by using methyl trimethoxysilane (MTMS, Shin-Etsu Chemical Co., Ltd.) and tetramethyl orthosilicate (TMOS > 98.0%, Junsei Chemical Co., Ltd.) as source materials. Those source materials were mixed with solvent with the molar ratio as $MTMS:TMOS:CH_3OH:H_2O:HCl = 0.5:0.5:2.4:1.3:1 \times 10^{-5}$. After hydrolysis at 50 °C for 3 h, the wet SiO_2 gels were obtained by adding NH_3 aqueous solution with a molar ratio of Si alkoxide:H_2O:$NH_3 = 1:2.7:6 \times 10^{-4}$. The obtained SiO_2 wet gels were aged in closed bottles at 35 °C for 5 days.

On the other hand, the (Al, Eu)-doped SiO_2 sols were prepared by two steps reactions. Firstly, Al-doped sols were prepared using tetraethyl orthosilicate (TEOS) and aluminum triethoxide ($Al(OC_2H_5)_3$) as source materials. Those source materials were mixed with solvent in the molar ratio of $TEOS:Al(OC_2H_5)_3:C_2H_5OH:H_2O:HNO_3:Eu(NO_3)_3 \cdot 6H_2O = 99:1:150:400:1.1:0.5$. After refluxing the sols composed of alkoxide and ethanol at 70 °C for 15 min followed by cooling down to ~25 °C, a mixture of Eu $(NO_3)_3 \cdot 6H_2O$, H_2O, C_2H_5OH, and HNO_3 was added to the sol, and the sol was stirred for 30 min. The homogenized sols were gelated, and the resultant wet gels were aged in ethanol at 50 °C for 5 days. Note that the gels with CH_3 groups and (Al, Eu)-doped gels are abbreviated by G–CH_3 and G–AE, hereafter. Further details of the gel preparation process have been published elsewhere [26, 27].

The wet gels, G–CH_3 and G–AE, were dried in CO_2 under supercritical condition using an autoclave to enhance the formation of pores on a mesoscale [28]. The autoclave with the wet gels was heated to 40 °C and filled with liquid CO_2, pressurized to 20 MPa. The temperature was, subsequently, raised to 80 °C at a rate of 1 °C/min to satisfy the supercritical conditions. After closing the valves, the temperature and pressure were maintained for 2 h. To remove the alcohol in the autoclave, the valves were opened, and CO_2 liquid continuously flowed into the autoclave. Finally, dried aerogels were obtained after gradual depressurization and cooling. The aerogels obtained from G–CH_3 and G–AE are abbreviated by AG–CH_3 and AG–AE, respectively.

The nitridation of the obtained gels was induced by ammonolysis using a conventional tube furnace. Fresh and pure NH_3 gas (99.999%, Showa Denko K.K.) continuously introduced into the furnace tube at a rate of 300 mL/min during whole ammonolysis process. The furnace temperature was held at a specified ammonolysis temperature (T_N) at between 750 and 1400 °C for 12 h after ramping at a rate of 1 °C/min. The samples prepared by ammonolysis at T_N from AG–CH_3 and AG–AE are represented by ON–CH_3 and ON–AE, respectively. For instance, the sample prepared by ammonolysis at 1000 °C from AG–CH_3 is abbreviated by ON–CH_3–1000 when T_N has to be specified.

2.1 Materials characterizations

Nitrogen adsorption–desorption isotherms of the aerogels, AG–CH_3 and AG–AE, were recorded at −196 °C by a gas adsorption analyzer (BELSORP-max, MicrotracBEL Corp.). The specific surface area, S_{BET}, was calculated by the Brunauer–Emmett–Teller (BET) method [29]. The pore size distribution was evaluated by Barret–Joyner–Halenda

(BJH) method [30] and non-local density functional theory (NLDFT) method [31] provided by instrument softwares (BELMaster^{TM} and BELSim^{TM}, MicrotracBEL Corp.).

The elemental composition of the ON–AE samples was analyzed by X-ray fluorescence spectroscopy (XRF, ZSX Primus II, Rigaku). On the other hand, the nitrogen concentration of the ON–CH_3 samples was determined using an oxygen/nitrogen analyzer (TC-436AR, LECO Japan Corp.). The crushed ON–CH_3 samples loaded into the equipment was heated in pure helium (He) gas to form a melt, and the N_2 gas desorbed from the sample was quantified with a thermal conductivity detector.

The atomic coordination in the aerogels and oxynitride glasses were investigated using NMR spectroscopy. High-resolution dipolar decoupling magic-angle spinning (DDMAS) method was adopted for ^{29}Si NMR at 99.38 MHz using a JEOL ECA 500 MHz spectrometer. The samples were packed in a 4 mm zirconia rotor and spun at a frequency of 10 kHz. The ^{29}Si DDMAS-NMR spectra were measured using a 3 µs of π/2 pulse width and a relaxation delay of 120 s. The ^{29}Si chemical shift was calibrated using tetramethylsilane as the external reference. For the AG–AE and ON–AE samples, the ^{27}Al magic-angle spinning (MAS) NMR signal at 208.49 MHz was measured using a JEOL ECZ 800 MHz spectrometer. The samples were spun in a 3.2 mm double-tuned broadband probe at 20 kHz. The ^{27}Al MAS-NMR spectra were collected with a pulse width of 0.6 µs, which was 1/3rd of π/2 (= 1.8 µs) in $AlCl_3$ aqueous solution and a 1.0 s relaxation delay. The chemical shift of ^{27}Al was calibrated with a reference, 1 mol% $AlCl_3$ aqueous solution, at 0 ppm.

3 Results and discussion

3.1 Gels

Figure 1(a) shows the N_2 adsorption–desorption isotherms of the dried aerogels, AG–CH_3 and AG–AE. The adsorption and desorption curves of both samples represent that the pores are IV type [32] and the adsorption and desorption amount of AG–CH_3 was larger than those of AG–AE in the whole range of relative pressure, *p/p0* range. The desorption amount of AG–AE changed abruptly at around $p/p0 = 0.7$, but the desorption of AG–CH_3 gradually decreased. The hysteresis loop of AG–AE assigned to Type H2(b) associated with pore blocking, which is typical for mesoporous inorganics materials such as mesoporous silicas, while that of AG–CH_3 resembles Type H3 suggesting pore network consisting of larger pores, which may relate with organic characteristics of AG–CH_3. Such difference in adsorption/desorption behavior of between AG–CH_3 and AG–AE indicates that the pores in AG–CH_3 has organic characteristics and those of AG–AE are inorganic ones [32]. As

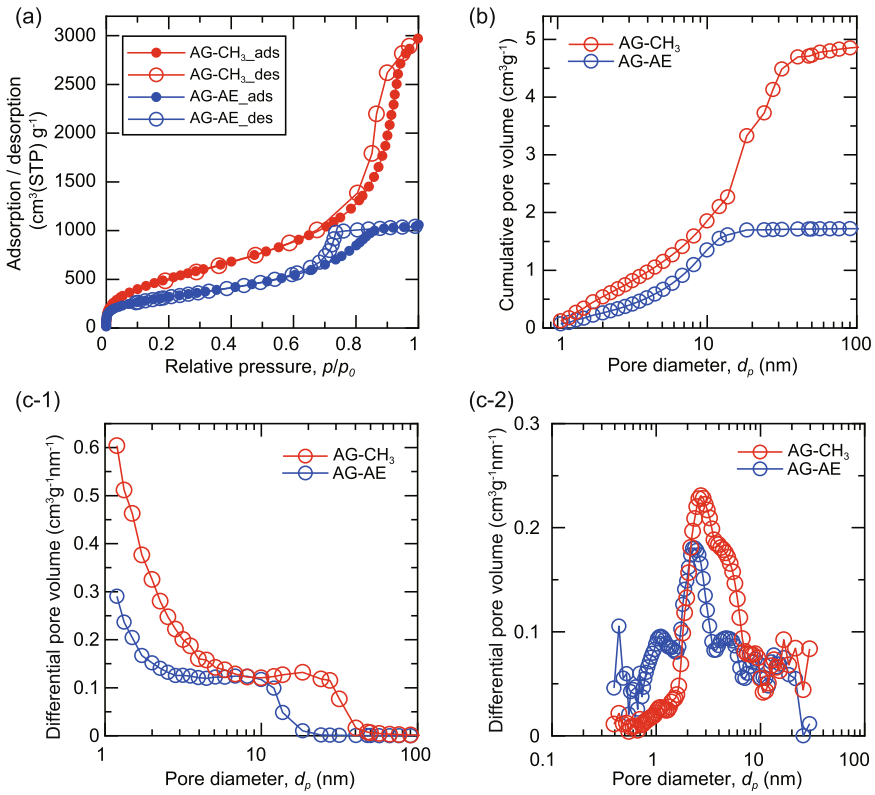

Fig. 1 **a** N_2 adsorption and desorption isotherms for the aerogels, AG–CH_3 and AG–AE, Closed circles represent the adsorption isotherms and open ones the desorption. **b** Cumulative pore volume, and (**c**) pore size distributions of the aerogels determined by (**c**-1) BJH method and (**c**-2) NLDFT method

Table 1 Specific surface area (S_{BET}), and pore volume (V_p) of the aerogels

	Specific surface area (S_{BET}/m^2g^{-1})	Pore volume (BJH) (V_p/$cm^3{\cdot}g^{-1}$)
AG-CH3	1941	4.96
AG-AE	1159	1.73

summarized in Table 1, the specific surface area of AG–CH_3 and AG–AE estimated by BET method was 1941 and 1159 $m^2\,g^{-1}$, respectively. The cumulative pore volume of the aerogels shown in Fig. 1(b) indicates that the total pore volume of AG–CH_3 is much larger than that of AG–AE and those pores with relatively large volume are formed in AG–CH_3. The pore size distribution estimated by BJH method is shown in Fig. 1(c-1). The largest pore size calculated by BJH method is 40 nm for AG-CH_3 and 20 nm for AG-AE. Both curves increased abruptly at pore size <4 nm although no obvious peak is found. The pore size distribution was also calculated by NLDFT method [31], because BJH method is, generally, not appropriate for smaller pores than 2 nm. As shown in Fig. 1(c-2), the pore size distribution of AG–CH_3 and of AG–AE has a peak at ~2.7 and 2.1 nm, respectively, which is consistent with abrupt increase of pore size distribution calculated by BJH method. In the case of AG–CH_3, there is a shoulder at around 5 nm, indicating that major/pore size in AG–CH_3 is two times smaller than that of AG–AE. Hence, the difference contribution of CH_3-modification and (Al, Eu)-doping upon pore volume and size distribution is clearly shown. The difference in pore volume and size distribution between AG–CH_3 and AG–AE likely relates to their cracking behavior during ammonolysis. Indeed, AG–AE was crushed by ammonolysis but monolithic oxynitride glasses were obtained from AG-CH_3 as mentioned above. In AG–CH_3, the incorporation of CH_3 groups originated in the source alkoxide may divide and terminate the silica networks.

3.2 Nitridation of the aerogels

As described in a previous report [26], the ON–CH_3 glasses, which were made from AG–CH_3 by ammonolysis, were not cracked and remained translucent even after ammonolysis. The bulk densities of ON–CH_3 were nearly unchanged with T_N at 750–1100 °C, and increased gradually with T_N over 1200 °C. On the other hand, ON–AE glasses, which were made from AG–AE, were crushed into chips during ammonolysis [27]. The relative nitrogen concentration in the samples after ammonolysis is shown in Fig. 2. In both of ON–CH_3 and ON–AE, the nitrogen concentration increased with T_N, but behavior was a little different from each other. For ON–AE, the nitrogen concentration monotonically increased with T_N and reached to over 38 eq.%. On the other hand, the nitrogen

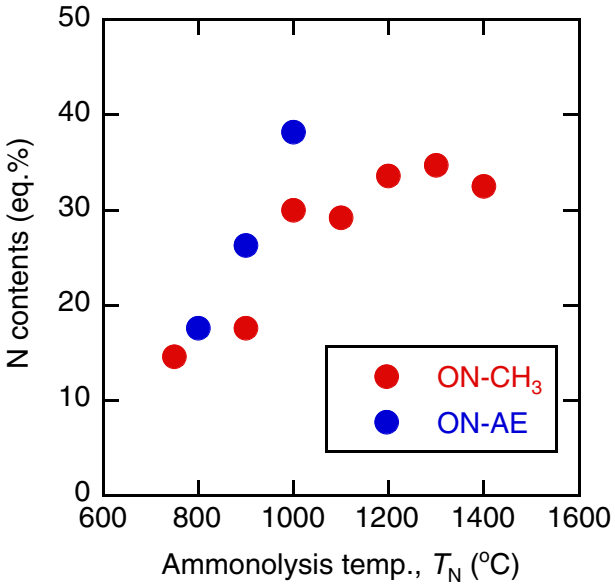

Fig. 2 Nitrogen concentration of the oxynitride glasses; red circles: ON–CH_3 and blue circles: ON–AE versus ammonolysis temperature

concentration in ON–CH_3 showed a jump at between $T_N = 900$ and 1000 °C, increased gradually at $T_N > 1000$ °C, and reached the maximum over 34 eq.%. The N equivalent contents represent simple substitution of nitrogen for oxygen. Thus, more than 35% oxygen atoms are substituted by nitrogen after ammonolysis at a relatively high temperature. The highest nitrogen concentration in ON–AE seemed to be a little higher compared to that of ON–CH_3.

Figure 3(a) shows ^{29}Si NMR spectra of AG–CH_3 and ON–CH_3. The modifications for the silicon-based tetrahedron; [SiX_4] (X = oxygen or organic groups, CH_3 in our case) are represented by "Q" and "T"; "Q^n" denotes a tetrahedron bonded to four oxygen, [SiO_4] and "T^n" denotes a tetrahedron bonded to three oxygen and one organic group, [$Si(CH_3)O_3$] in our case, where n means the number of bridging oxygen atoms shared by two neighboring [SiX_4] tetrahedrons [33, 34]. All those spectra have a peak at around −110 ppm. In general, SiO_2 glass has a network structure composed of corner shared [SiO_4] tetrahedra. Namely, all four oxygen of each [SiO_4] tetrahedron bridges another tetrahedron, and such Si atoms are represented by Q^4. Typical chemical shift for Q^4 units is known to be −107 ppm in ^{29}Si NMR [35, 36]. Hence, the peak at −110 ppm is assignable to Q^4. The peak for Q^4 units was obviously seen in all spectra for ON–CH_3 samples even after ammonolysis at high temperature. In AG-CH_3, two peaks appear in the range at −66 to −56 ppm. The main peak at −63 ppm is assigned to T^3, [$Si(CH_3)(OSi\equiv)_3$] and the peak at −56 ppm is assigned to T^2, $Si(CH_3)(OSi\equiv)_2(OX)$ (X = H or CH_3) [37, 38]. The peaks assigned to T^3 and T^2 was originated by MTMS in the aerogel. However,

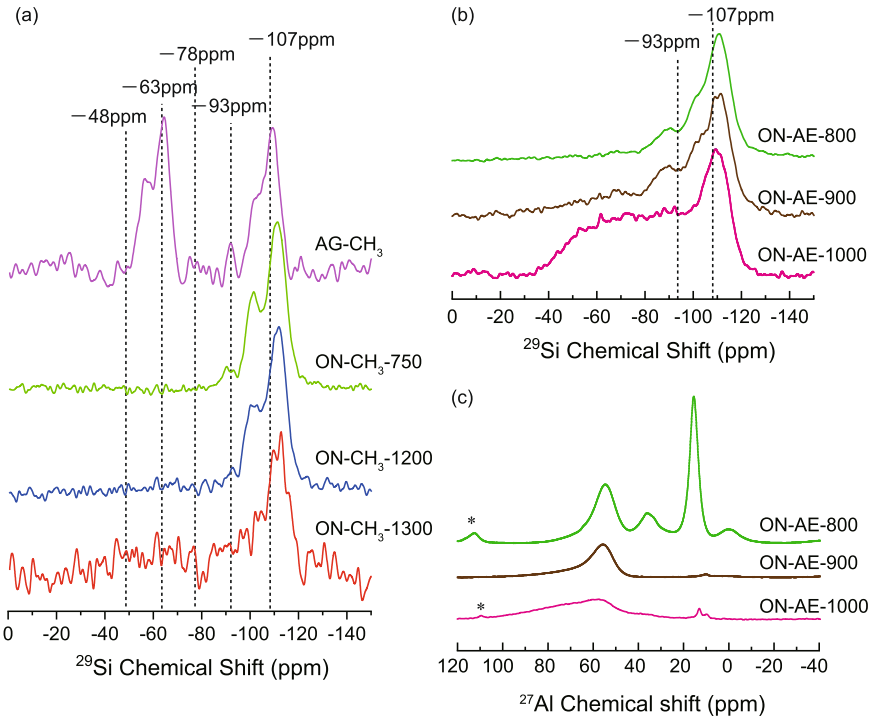

Fig. 3 ^{29}Si NMR spectra of (**a**) AG − CH_3 and ON − CH_3 and (**b**) ON − AE samples. **c** ^{27}Al NMR spectra of ON − AE samples. *:spinning side band

the spectral feature assignable to T^3 and T^2 was not found even in ON–CH_3–750, which was prepared at the lowest T_N among the samples prepared in this study. As FTIR spectrum of ON–CH_3 did/not exhibited any features assignable to Si-C bonds [26], we can safely conclude that Si-C bonds, T^3 and T^2 feature, did not exist in ON–CH_3 samples.

Variation of chemical shift in ^{29}Si NMR spectra due to nitrogen substitution in [SiO_4] tetrahedron has been reported to be approximately −15 ppm per one nitrogen such as [SiO_4]: −107 ppm, [$SiNO_3$]: −93 ppm, [SiN_2O_2]: −78 ppm, [SiN_3O]: −63 ppm and [SiN_4]: −48 ppm [35]. In the NMR spectra of ON–CH_3–750 and ON–CH_3–1200, there is a small peak at around −93 ppm, indicating that [$SiNO_3$] unit is formed. In the spectrum for ON–CH_3–1200, a broad signal appears in the range of −40 to −80 ppm. This broad signal can be attributed to the presence of [SiN_2O_2], [SiN_3O] and [SiN_4]. In the spectrum for ON–CH_3–1300, a broad signal is further clearly seen in the range from −40 to −80 ppm. Those results are reasonable because the nitrogen concentration in ON–CH_3 increased with the increase of T_N as mentioned above. It is also notable that the peak intensity for Q^4 was weak for ON–CH_3–1300, indicating that population of [SiO_4] tetrahedra decreased with the increase of nitrogen concentration at higher T_N. The peak position of Q^4 shifted to high magnetic field side with increase of the T_N. The increase of shielding suggests that the introduction of nitrogen substituted for oxygen causes an increase in the covalency of the chemical bonding surrounding Si atoms [33, 39].

A shoulder at around −100 ppm for the peak attributed to Q^4 structure is also found in ^{29}Si NMR spectra of AG-CH_3 and ON–CH_3, and the intensity of this peak decreased with increase of T_N. Looking at literatures, this peak can be assigned to Q^3, particularly originated in [$Si(OH)O_3$], where one of oxide ion of [SiO_4] tetrahedra is replaced by an OH group [35, 38]. With this assignment, the observed results indicated that OH groups are coordinated to Si but the concentration of Si-OH components decreases with increasing T_N. As the decomposition of ammonia results in high hydrogen partial pressure, the hydrogen incorporation during ammonolysis is a possible explanation. It is also possible that the decomposition of residual solvents or CH_3 groups in the gel caused the hydrogen incorporation in the glass during heat treatment. As the shoulder at around −100 ppm is not pronounced in the spectrum for ON–CH_3–1300, not incorporation but desorption of hydrogen is likely favorable at higher temperatures.

The spectra of ^{29}Si NMR of ON–AE are shown in Fig. 3(b). A peak at approximately −110 ppm, which is assignable to Q^4 species, are found in all ON–AE samples as similar to ON–CH_3. In ON–AE–800 and ON–AE–900, a spectral shoulder at −100 ppm and peak at around −90 ppm can be found, but the shoulder at −100 ppm was not evident in ON–AE–1000. The shoulder at around −100 ppm is assignable to Q^3 structure with one OH ligand as similar to ON–CH_3, and this is also an indication that the desorption of hydrogen is more favorable at higher temperatures. The peak at −90 ppm can be identified as a peak originated in [$SiNO_3$] coordination as similar to the case for ON–CH_3.

In addition, there is a broad band at around −40 to −70 ppm in the ^{29}Si NMR spectrum for ON–AE–900, and the intensity of the band was obviously enhanced in ON–AE–1000. Huge enhancement of the broad band for ON–AE–1000 resulted in overlapping of the broad band and peaks in the range from −90 to −100 ppm. Here, the identification of the shoulder at −100 ppm must be discussed. As described above, the shoulder at −100 ppm found for the ON-CH_3 samples prepared at relatively low T_N is assignable to [$Si(OH)O_3$] units. However, in a literature [36], the shoulder at −100 ppm has been attributed to $Si(OSi)_3(OAl)$ structure where one of four oxygens in a [SiO_4] octahedron is bonded to Al. Therefore, the shoulder at −100 ppm in ON-AE samples may be attributed to $Si(OSi)_3(OAl)$. However, because of the overlapping of very broad signal, a clear peak originated in $Si(OSi)_3(OAl)$ structure was not detected. As Al concentration in ON-AE is very low, the absence of a peak originated in Al substitution is very reasonable. The most probable explanation for the presence of the broad signal is nitrogen incorporation. As mentioned above, the signal at the range from −40 to −80 ppm is attributed to [$SiNO_3$], [SiN_2O_2], [SiN_3O] and [SiN_4] [35, 40, 41]. As the nitrogen concentration increased three times with the increase of T_N from 800 to 1000 °C in ON-AE (Fig. 2), the very broad signal extended in the range from −40 to −80 ppm is attributed to [SiN_mO_{4-m}] structures with $m > 1$.

The ^{27}Al NMR spectra of ON-AE samples are shown in Fig. 3(c). The ^{27}Al NMR spectra exhibit the chemical shift depending on the coordination number of Al. The peaks at 55 ppm are assigned to fourfold coordinated Al, [4] Al [42]. In ON-AE after nitridation at 900 and 1000 °C, only one evident peak at around 55 ppm appeared, indicating that almost all Al forms [AlO_4] tetrahedra in the glass network. This band at 55 ppm for ON–AE–1000 was broader than that for ON–AE–900. On the other hand, other three peaks at around 35, 15 and 0 ppm were found in ON–AE–800. The peak at 35 ppm is also assigned to [4] Al, which is distorted AlO_4^- sites in tricluster tetrahedra; three AlO_4 tetrahedra sharing a common oxygen atom observed in mullite [43, 44]. The peaks at 15 and 0 ppm can be assigned to [6] Al [42–45] which is for Al involved in a [AlO_6] octahedron. The NMR spectra represent that the surrounding of Al changed drastically from 800 to 900 °C and the [AlO_4] unit was formed in the glass network by the nitridation at the temperature higher than 900 °C.

3.3 Crack generation

The impact of CH_3–modification upon aerogel structure can be attributed to the termination of the network composed of [SiO_4] tetrahedra. That is evidenced by the adsorption/desorption curve shown in Fig. 1(a): those behavior indicated that the surface of AG–CH_3 possesses more organic characteristics compared to AG–AE. The larger pore volume is likely resulting from the termination of the network structure. As mentioned, no trace of the structures related to the organic component, CH_3, was observed in ON–CH_3 even after ammonolysis at 750 °C, which suggests that the crack generation during ammonolysis was not directly relating to the presence of CH_3 groups. That means that microscopic or mesoscopic structure in AG–CH_3 composed of shredded [SiO_4] network was memorable during ammonolysis, which are two possible understandings. One is that recovery from shredded [SiO_4] glass network or relaxation of mesoscopic structure takes relatively long relaxation time. This may be a reason for inhibition of crack generation in ON–CH_3 during ammonolysis. The other is relatively quick nitrogen diffusion during ammonolysis, since it is presumable that nitrogen diffuse into aerogel before relaxation of the shredded [SiO_4] network. Tentatively, it is presumed that either or both of those mechanism works to prevent crack generation in ON–CH_3 during ammonolysis.

On the other hand, looking at ^{27}Al NMR spectrum of ON–AE–800, it seems that local structure around Al was distorted in the aerogel and not completely relaxed even after ammonolysis at 800 °C. That means that distorted structure was introduced in AG–AE. In addition, presence of [$Si(OH)O_3$] was suggested in both ON–CH_3 and ON–AE prepared with relatively low T_N. However, the ON–AE samples were crushed during ammonolysis and monolithic ON-AE could not be obtained. Hence, the role of (Al, Eu)-doping and CH_3–modification should be regarded as different role and that presence of [$Si(OH)O_3$] is unlikely a solid reason for inhibition of crack generation. Hence, the most probable reason for successful synthesis of monolithic oxynitride glass in ON–CH_3 series is formation of relatively large pores in mesoscale range. It is an important indication for our future study on synthesis of monolithic oxynitride glasses. That is controlling of mesoscale structure, which affects to kinetics of nitrogen in cooperation and stress relaxation, is a key for inhibition of cracking.

3.4 Charge compensation

Charge compensation in oxynitride glasses is the most important issue in the fundamental part of glass science. As formal charge of oxygen and nitrogen differs, we need to explain charge compensation mechanism. In terms of formal charge, formation of a hydrogen–nitrogen ([N^{3-}–H^+]) pair is a possible charge compensation when nitrogen substitute for oxygen (O^{2-}). On this assumption, combination of [$Si(OH)O_3$] with [$SiNO_3$] is likely a way of charge compensation. However, fraction of [$Si(OH)O_3$] seemingly reduced at high T_N, although concentration of nitrogen

increases with T_N. Therefore, the oxynitride prepared with high T_N has to satisfy charge neutrality by replacing three O^{2-} by two N^{3-}. Namely, total number of anion (sum of the number of oxygen and nitrogen) should decrease with the increase of nitrogen concentration.

4 Conclusions

Silicone oxynitride, Si-O-N, and Si-Al-O-N glasses were prepared from oxide aerogels via ammonolysis at temperatures from 750 to 1400 °C. The SiO_2 gels were prepared from TMOS and MTMS with CH_3 groups, the SiO_2-Al_2O_3 gels were prepared from TEOS and $Al(OC_2H_5)_3$, and the gels were dried in supercritical CO_2, resulting in the formation of aerogels. The specific surface area of these aerogels was 1941 and 1159 $m^2 g^{-1}$. The nitrogen was inserted in these aerogels by ammonolysis, and the amount of nitrogen increased with an increase of the ammonolysis temperature and exceeded 34 eq.%. The structures of the oxynitride glasses were characterized using ^{29}Si and ^{27}Al NMR spectra. In Si-O-N glasses, the Si atoms bonded to one nitrogen atom are formed at temperatures lower than 1200 °C and the Si atoms bonded to two or more nitrogen atoms are formed at temperatures higher than 1300 °C. In Si-Al-O-N glasses, the N atom is bonded not to Al but to Si atoms, and various numbers of N atoms are bonded to a Si atom by the ammonolysis at 1000 °C.

Acknowledgements This work was supported by the MEXT Elements Strategy Initiative to Form Core Research Center for Electronic Materials: Tokodai Institute of Elements Strategy, Japan, Grant Number JPMXP0112101001.

Compliance with ethical standards

Conflict of interest The authors declare no competing interests.

Publisher's note Springer Nature remains neutral with regard to jurisdictional claims in published maps and institutional affiliations.

References

1. Sakka S (1995) Structure, Properties and Application of Oxynitride Glasses. J Non-Cryst Solids 181:215–224. https://doi.org/10.1016/S0022-3093(94)00514-1
2. Hampshire S (2003) Oxynitride glasses, their properties and crystallisation – a review. J Non-Cryst Solids 316:64–73. https://doi.org/10.1016/s0022-3093(02)01938-5
3. Hampshire S, Pomeroy MJ (2008) Oxynitride Glasses. Int J Appl Ceram Technol 5:155–163. https://doi.org/10.1111/j.1744-7402.2008.02205.x
4. Ali S, Jonson B, Pomeroy MJ, Hampshire S (2015) Issues associated with the development of transparent oxynitride glasses. Ceram Int 41:3345–3354. https://doi.org/10.1016/j.ceramint.2014.11.030
5. Garcia ÀR, Clausell C, Barba A (2016) Oxynitride glasses: a review. Boletín de la Soc Española de Cerámica y Vidr 55:209–218. https://doi.org/10.1016/j.bsecv.2016.09.004
6. Hakeem AS, Ali S, Jonson B (2013) Preparation and properties of mixed La–Pr silicate oxynitride glasses. J Non-Cryst Solids 368:93–97. https://doi.org/10.1016/j.jnoncrysol.2013.03.013
7. Hakeem AS, Daucé R, Leonova E, Edén M, Shen Z, Grins J, Esmaeilzadeh S (2005) Silicate Glasses with Unprecedented High Nitrogen and Electropositive Metal Contents Obtained by Using Metals as Precursors. Adv Mater 17:2214–2216. https://doi.org/10.1002/adma.200500715
8. Ali S, Jonson B, Rouxel T (2011) Glasses in the Ba-Si-O-N System. J Am Ceram Soc 94:2912–2917. https://doi.org/10.1111/j.1551-2916.2011.04718.x
9. Ali S, Jonson B (2011) Compositional effects on the properties of high nitrogen content alkaline-earth silicon oxynitride glasses, AE=Mg, Ca, Sr, Ba. J Eur Ceram Soc 31:611–618. https://doi.org/10.1016/j.jeurceramsoc.2010.11.005
10. Loehman RE (1983) Preparation and Properties of Oxynitride Glasses. J Non-Cryst Solids 56:123–134. https://doi.org/10.1016/0022-3093(83)90457-X
11. Brinker CJ, Haaland DM (1983) Oxynitride Glass-Formation from Gels. J Am Ceram Soc 66:758–765. https://doi.org/10.1111/j.1151-2916.1983.tb10558.x
12. Rajaram M, Day DE (1987) Nitrogen Dissolution in Sodium Alkaline-Earth Metaphosphate Melts. J Am Ceram Soc 70:203–207. https://doi.org/10.1111/j.1151-2916.1987.tb04968.x
13. Brinker CJ, Haaland DM, Loehman RE (1983) Oxynitride Glasses Prepared from Gels and Melts. J Non-Cryst Solids 56:179–184. https://doi.org/10.1016/0022-3093(83)90465-9
14. Kamiya K, Ohya M, Yoko T (1986) Nitrogen-Containing SiO_2 Glass-Fibers Prepared by Ammonolysis of Gels Made from Silicon Alkoxides. J Non-Cryst Solids 83:208–222. https://doi.org/10.1016/0022-3093(86)90068-2
15. Brow RK, Pantano CG (1987) Thermochemical Nitridation of Microporous Silica Films in Ammonia. J Am Ceram Soc 70:9–14. https://doi.org/10.1111/j.1151-2916.1987.tb04845.x
16. Brinker CJ, Scherer GW (1990) Sol-gel science: the physics and chemistry of sol-gel processing. Academic Press, San Diego
17. Szaniawska K, Murawski L, Pastuszak R, Walewski M, Fantozzi G (2001) Nitridation and densification of SiO_2 aerogels. J Non-Cryst Solids 286:58–63. https://doi.org/10.1016/S0022-3093(01)00478-1
18. Szaniawska K, Gładkowski M, Wicikowski L, Murawski L (2008) Nitridation of SiO2–B2O3 aerogels. J Non-Cryst Solids 354:4481–4483. https://doi.org/10.1016/j.jnoncrysol.2008.06.072
19. Ahmadi S, Eftekhari Yekta B, sarpoolaky H, Aghaei A (2014) Preparation of monolithic oxynitride glasses by sol–gel method. J Non-Cryst Solids 404:61–66. https://doi.org/10.1016/j.jnoncrysol.2014.07.037
20. Kistler SS (1931) Coherent Expanded Aerogels and Jellies. Nature 127:741–741. https://doi.org/10.1038/127741a0
21. Prakash SS, Brinker CJ, Hurd AJ, Rao SM (1995) Silica aerogel films prepared at ambient pressure by using surface derivatization to induce reversible drying shrinkage. Nature 374:439–443. https://doi.org/10.1038/374439a0
22. Yokogawa H, Yokoyama M (1995) Hydrophobic Silica Aerogels. J Non-Cryst Solids 186:23–29. https://doi.org/10.1016/0022-3093(95)00086-0

23. Kanamori K, Aizawa M, Nakanishi K, Hanada T (2007) New Transparent Methylsilsesquioxane Aerogels and Xerogels with Improved Mechanical Properties. Adv Mater 19:1589–1593. https://doi.org/10.1002/adma.200602457
24. Hernandez C, Pierre AC (2001) Evolution of the texture and structure of SiO_2-Al_2O_3 xerogels and aerogels as a function of the Si to Al molar ratio. J Sol-Gel Sci Technol 20:227–243. https://doi.org/10.1023/A:1008714617174
25. Woignier T, Phalippou J, Despetis F, Calas-Etienne S (2018) In: Klein L et al. (ed) Handbook of Sol-Gel Science and Technology, Springer International Publishing AG, part of Springer Nature. https://doi.org/10.1007/978-3-319-32101-1_27
26. Osawa Y, Iwasaki K, Nakanishi T, Yasumori A, Matsui Y, Nishimura T, Ohsawa T, Segawa H, Ohashi N (2021) Synthesis of bulk silicon oxynitride glass through nitridation of SiO_2 aerogels and determination of T_g. J Am Ceram Soc 104:4420–4432. https://doi.org/10.1111/jace.17836
27. Watanabe S, Osawa Y, Machida S, Katsumata K-i, Yasumori A, Takahashi K, Deguchi K, Ohki S, Segawa H (2021) Investigation of luminescence properties of Eu-doped Si-Al-O-N glasses synthesized via sol-gel process. J Non-Cryst Solids 573. https://doi.org/10.1016/j.jnoncrysol.2021.121107
28. Segawa H, Ohki S, Deguchi K, Shimizu T, Hirosaki N (2020) Exploration of zinc borophosphate glasses as dispersion media for SiAlON phosphors. Int J Appl Glass Sci 11:471–479. https://doi.org/10.1111/ijag.15004
29. Brunauer S, Emmett PH, Teller E (1938) Adsorption of gases in multimolecular layers. J Am Chem Soc 60:309–319. https://doi.org/10.1021/ja01269a023
30. Barrett EP, Joyner LG, Halenda PP (1951) The Determination of Pore Volume and Area Distributions in Porous Substances. I. Computations from Nitrogen Isotherms. J Am Chem Soc 73:373–380. https://doi.org/10.1021/ja01145a126
31. Landers J, Gor GY, Neimark AV (2013) Density functional theory methods for characterization of porous materials. Colloids Surf A: Physicochemical Eng Asp 437:3–32. https://doi.org/10.1016/j.colsurfa.2013.01.007
32. Thommes M, Kaneko K, Neimark AV, Olivier JP, Rodriguez-Reinoso F, Rouquerol J, Sing KSW (2015) Physisorption of gases, with special reference to the evaluation of surface area and pore size distribution (IUPAC Technical Report. Pure Appl Chem 87:1051–1069. https://doi.org/10.1515/pac-2014-1117
33. Maekawa H, Maekawa T, Kawamura K, Yokokawa T (1991) The structural groups of alkali silicate glasses determined from ^{29}Si MAS-NMR. J Non-Cryst Solids 127:53–64. https://doi.org/10.1016/0022-3093(91)90400-z
34. Nanba T, Nishimura M, Miura Y (2004) A theoretical interpretation of the chemical shift of ^{29}Si NMR peaks in alkali borosilicate glasses. Geochim Cosmochim Acta 68:5103–5111. https://doi.org/10.1016/j.gca.2004.05.042
35. Weeren R, Leone EA, Curran S, Klein LC, Danforth SC (1994) Synthesis and Characterization of Amorphous Si_2N_2O. J Am Ceram Soc 77:2699–2702. https://doi.org/10.1111/j.1151-2916.1994.tb04664.x
36. Dogan F, Hammond KD, Tompsett GA, Huo H, Conner Jr. WC, Auerbach SM, Grey CP (2009) Searching for microporous, strongly basic catalysts: experimental and calculated ^{29}Si NMR spectra of heavily nitrogen-doped Y zeolites. J Am Chem Soc 131:11062–11079. https://doi.org/10.1021/ja9031133
37. El Rassy H, Pierre AC (2005) NMR and IR spectroscopy of silica aerogels with different hydrophobic characteristics. J Non-Cryst Solids 351:1603–1610. https://doi.org/10.1016/j.jnoncrysol.2005.03.048
38. Borba A, Vareda JP, Durães L, Portugal A, Simões PN (2017) Spectroscopic characterization of silica aerogels prepared using several precursors – effect on the formation of molecular clusters. N J Chem 41:6742–6759. https://doi.org/10.1039/c7nj01082f
39. Leonova E, Hakeem AS, Jansson K, Stevensson B, Shen Z, Grins J, Esmaeilzadeh S, Edén M (2008) Nitrogen-rich La–Si–Al–O–N oxynitride glass structures probed by solid state NMR. J Non-Cryst Solids 354:49–60. https://doi.org/10.1016/j.jnoncrysol.2007.07.027
40. Carduner KR, Carter RO, Milberg ME, Crosbie GM (1987) Determination of phase composition of silicon nitride powders by silicon-29 magic angle spinning nuclear magnetic resonance spectroscopy. Anal Chem 59:2794–2797. https://doi.org/10.1021/ac00150a015
41. Chollon G, Hany R, Vogt U, Berroth K (1998) A silicon-29 MAS-NMR study of alpha-silicon nitride and amorphous silicon oxynitride fibres. J Eur Ceram Soc 18:535–541. https://doi.org/10.1016/S0955-2219(97)00162-3
42. Sen S, Xu Z, Stebbins JF (1998) Temperature dependent structural changes in borate, borosilicate and boroaluminate liquids: high-resolution ^{11}B, ^{29}Si and ^{27}Al NMR studies. J Non-Cryst Solids 226:29–40. https://doi.org/10.1016/s0022-3093(97)00491-2
43. Walkley B, Rees GJ, San Nicolas R, van Deventer JSJ, Hanna JV, Provis JL (2018) New Structural Model of Hydrous Sodium Aluminosilicate Gels and the Role of Charge-Balancing Extra-Framework Al. J Phys Chem C 122:5673–5685. https://doi.org/10.1021/acs.jpcc.8b00259
44. Rehak P, Kunath-Fandrei G, Losso P, Hildmann B, Schneider H, Jager C (1998) Study of the Al coordination in mullites with varying Al: Si ratio by Al-27 NMR spectroscopy and X-ray diffraction. Am Miner 83:1266–1276. https://doi.org/10.2138/am-1998-11-1215
45. Poe BT, McMillan PF, Angell CA, Sato RK (1992) Al and Si coordination in SiO_2-Al_2O_3 glasses and liquids: a study by NMR and IR spectroscopy and MD simulations. Chem Geol 96:333–349. https://doi.org/10.1016/0009-2541(92)90063-b